Biomaterials 30 (2009) 902–909

Contents lists available at ScienceDirect

Biomaterials

journal homepage: www.elsevier.com/locate/biomaterials

BSA-FITC-loaded microcapsules for *in vivo* delivery

Byung Soo Kim [a], Jae Min Oh [a,b], Kyung Sook Kim [a], Kwang Soo Seo [a], Jae Song Cho [a,b], Gilson Khang [b], Hai Bang Lee [a,**], Kinam Park [c,**], Moon Suk Kim [a,*]

[a] Fusion Biotechnology Research Center, Korea Research Institute of Chemical Technology, PO Box 107, Yuseong, Daejeon 305-600, South Korea
[b] BK-21 Polymer BIN Fusion Research Team, Chonbuk National University, 664-14, Dukjin Dong 1Ga, Dukjin Ku, Jeonju 561-756, South Korea
[c] Departments of Biomedical Engineering and Pharmaceutics, Purdue University, 206 S. Intramural Drive, West Lafayette, IN 47907-1791, USA

ARTICLE INFO

Article history:
Received 25 September 2008
Accepted 21 October 2008
Available online 22 November 2008

Keywords:
Microcapsule
Ultrasonic atomizer
BSA
Sustain
Inflammation

ABSTRACT

Here we describe the preparation of BSA-FITC-loaded microcapsules as a model protein system for *in vivo* delivery. BSA-FITC-loaded microcapsules were prepared using a mono-axial nozzle ultrasonic atomizer, varying a number of parameters to determine optimal conditions. The preparation method chosen resulted in a BSA-FITC encapsulation efficiency of ~60% and a particle size of ~50 μm. An analysis of the microcapsules showed a BSA-FITC core surrounded by a poly(D,L-lactic-co-glycolic acid) (PLGA) shell. Injection of BSA-FITC-loaded microcapsules into rats resulted in a sustained release of BSA-FITC that maintained increased concentrations of BSA-FITC in plasma for up to 2 weeks. In contrast, the concentration of BSA-FITC in plasma after injection of BSA-FITC-only solution reached near-zero levels within 3 days. Fluorescence images of microcapsules removed at various times after implantation showed a gradual decrease of BSA-FITC in BSA-FITC-loaded microcapsules, confirming a sustained *in vivo* release of BSA-FITC. The duration of *in vivo* release and plasma concentration of BSA-FITC was correlated with the initial dose of BSA-FITC. BSA-FITC-loaded microcapsules maintained their structure for at least 4 weeks in the rat. The inflammatory response observed initially after injection declined over time. In conclusion, BSA-FITC-loaded microcapsules achieved sustained release of BSA-FITC, suggesting that microcapsules manufactured as described may be useful for *in vivo* delivery of pharmacologically active proteins.

1. Introduction

In general, protein drugs exhibit poor bioavailability [1]. To improve the bioavailability of protein drugs, considerable effort has been devoted to the control and maintenance of long-term *in vivo* release, exploiting several administration routes, including oral administration, and pulmonary and parenteral injection [2]. In addition to improving bioavailability, long-term protein delivery, ranging from days to weeks, can decrease the frequency of protein administration and increase patient compliance [2,3]. Among the administration methods that have been developed, microencapsulation has been shown to improve protein stability and have the capacity to selectively entrap proteins in a polymer matrix [4–6]. Thus, a sustained protein drug-delivery system using a microcapsule depot offers a number of potentially important clinical advantages, including significantly reduced dosage frequency and improved efficacy without toxicity [7–9]. When used *in vivo*, microcapsules can also prevent immune recognition of the encapsulated protein, thus overcoming a major impediment to protein longevity. A microcapsule delivery system requires that particle sizes be less than 100 μm in diameter. This is because particles in this size range tend to remain at the injection site after subcutaneous or intramuscular administration, where they cause less pain and slowly release their drug contents over time [10,11].

To date, a number of microencapsulation techniques have been developed to entrap proteins into microcapsules, including double emulsion, organic phase separation, supercritical fluid and spray drying techniques [12–14]. One conventional method used to prepare protein-loaded microcapsules is the double emulsion-solvent extraction/evaporation method [15]. However, double emulsions are usually prepared by mechanical stirring, homogenization or ultrasonication, which can damage or destroy protein function. These methods also do not provide for fine control of particle size, and thus tend to yield microcapsules with a very broad size distribution. This lack of uniformity can cause a number of problems, including (1) lower bioavailability *in vivo* because only

* Corresponding author. Tel.: +82 42 860 7095; fax: +82 42 860 7228.
** Corresponding authors.
E-mail addresses: hblee@krict.re.kr (H.B. Lee), kpark@purdue.edu (K. Park), mskim@krict.re.kr (M.S. Kim).

0142-9612/$ – see front matter © 2008 Elsevier Ltd. All rights reserved.
doi:10.1016/j.biomaterials.2008.10.030

microcapsules within a certain size range can be used; (2) lower drug encapsulation efficiency; and (3) poor reproducibility. In addition, the harsh conditions that can occur during the microencapsulation process, which are often antithetical to protein stability, make it difficult to maintain the functional integrity of encapsulated proteins.

There is thus a need to develop new microencapsulation techniques that are capable of encapsulating proteins using simple procedures and mild conditions, thereby reducing the exposure of encapsulated proteins to deleterious environments [16,17]. Several new strategies have been developed to improve protein microencapsulation. Recently, a co-axial ultrasonic atomizer was shown to be a simple and highly efficient means of generating reservoir-type microcapsules using mild conditions [18–20]. The prepared microcapsules are spherical and small in size, offering optimal surface-to-volume ratio and diffusion capacity. At least with respect to short exposure to stressful conditions, the proteins microencapsulated by this method are more stable than those encapsulated by conventional methods. Following the successful application of the co-axial nozzle ultrasonic atomizer, several factors appear to influence the formation of complete microcapsules. From these studies, the use of a mono-axial nozzle ultrasonic atomizer may represent a potentially significant technological advance in the continuing effort to encapsulate stable proteins into microcapsules. This work addresses the various advantages for facilitating the formation of uniform microcapsules with a shell completely encapsulating the core. However, efficient fabrication of such microcapsules by specifically examining variation of the fabrication parameters has not been previously reported to our knowledge.

In this study, we used a mono-axial nozzle ultrasonic atomizer to prepare bovine serum albumin-fluorescein isothiocyanate (BSA-FITC)-loaded microcapsules. Our first objective was to develop a simple procedure to prepare protein-loaded microcapsules with desirable properties using BSA-FITC as the model protein, with a goal of improving drug encapsulation efficiency. The second aim of this study was to evaluate the activity of BSA-FITC-loaded microcapsules *in vivo* by administering them subcutaneously in rats. Finally, we assessed the duration of BSA-FITC release and host tissue response to determine whether BSA-FITC-loaded microcapsules could be used for sustained *in vivo* protein delivery.

2. Experimental

2.1. Materials

Low molecular weight poly(D,L-lactic-co-glycolic acid) (PLGA, lactic/glycolic acid = 50/50, MW = 14,500) was purchased from Birmingham Polymers, Inc. (Birmingham, AL). Poly(vinyl alcohol) (PVA, 87–89% hydrolyzed, MW = 85,000–124,000) purchased from Sigma (Milwaukee, WI) was used as an emulsifier. Fluorescein isothiocyanate (FITC)-labeled BSA and Nile Red were purchased from Sigma (St. Louis, MO). All other chemicals were analytical grades and used without further purification.

2.2. Microencapsulation of BSA-FITC using mono-axial nozzle ultrasonic atomizer

Microcapsules were generated by using a mono-axial nozzle ultrasonic atomizer (Sono-Tek Corp, Milton, NY). Various parameters were tried to manufacture microcapsule at optimized condition (Table 1). The preparation of F-6 formulation was as follow. A PLGA solution in ethyl acetate and an aqueous solution containing BSA-FITC were separately fed into an ultrasonic atomizer. The flow rates of the PLGA solution and the BSA-FITC aqueous solution were 4 and 0.2 mL/min, respectively. The concentrations of polymer and BSA-FITC were 3 and 5% (w/v), respectively. Microdroplets were produced by atomizing of the mixed solutions of PLGA and BSA-FITC for approximately 5 s at a vibration frequency of 3 W, 60 kHz, and they were then immediately collected in a 0.5% (w/v) PVA solution for 2 min. The distance between atomizer head and the aqueous PVA solution was 1 cm, and the stirring speed of the PVA solution was 1000 rpm. The resulting solutions were left with gentle stirring for 2 h to allow solidification of microcapsules, followed by washing with distilled water. The solution is frozen at −74 °C, followed by freeze-drying for 4–7 days. The morphology of obtained microcapsules was observed using CAMSCOPE (Sometech, Korea) and an optical microscope (Nikon, Labophot-2, Japan). The particle sizes of microcapsules were measured by Particle Size Analyzer (BI-DCP Particle Sizer, UK).

Table 1
Preparation of BSA-FITC loaded microcapsules.

No.	Flow rate (mL/min)		PVA (%)	PLGA (%)	Sonication (W)	Yield (%)	Encapsulation (%)	Size (μm)
	Polymer	BSA-FITC						
F-1	1	0.2	0.5	3	3	86	21	447
F-2	2	0.2	0.5	3	3	94	47	600
F-3	3	0.2	0.5	3	3	~100	50	631
F-4	4	0.2	0.5	3	2	95	59	400
F-5	4	0.2	0.5	1	3	91	27	465
F-6	4	0.2	0.5	3	3	92	63	48
F-7	4	0.2	0.5	5	3	94	74	491
F-8	4	0.2	0.5	10	3	83	71	12
F-9	4	0.2	1.0	3	3	84	66	27
F-10	4	0.2	2.0	3	3	83	49	28
F-11	4	0.2	0.5	3	4	93	61	76
F-12	4	0.2	0.5	3	5	90	40	48
F-13	4	0.2	0.5	3	6	93	40	52
F-14	4	0.2	0.5	3	7	~100	44	79
F-15	4	0.4	0.5	3	3	89	38	20
F-16	4	0.8	0.5	3	3	84	30	24
F-17	5	0.2	0.5	3	3	88	41	32
F-18	6	0.2	0.5	3	3	90	61	33
F-19	7	0.2	0.5	3	3	73	45	26

2.3. Confocal fluorescence microscopy (CFM)

For the sample preparation, BSA-FITC-loaded microcapsules were produced using 5% (w/v) BSA-FITC in aqueous solution and 0.003% Nile Red in the 3% (w/v) PLGA solution in ethyl acetate. Before the measurement, they were thoroughly washed with distilled water. The structure of the BSA-FITC-loaded microcapsule was examined using a laser scanning confocal imaging system (model LSM-510 Pascal, Carl Zeiss, Germany) equipped with a Argon/HeNe laser and a Zeiss LSM 510 inverted microscope. All confocal fluorescence pictures for BSA-FITC and Nile Red were taken with a ×20 objective lens and excitation at 488 and 568 nm, respectively.

2.4. Encapsulation efficiency of BSA-FITC-loaded microcapsules

The encapsulation efficiency of BSA-FITC was determined using CH_2Cl_2 and distilled water. Microcapsules (10 mg) were placed into a test tube to which CH_2Cl_2 (0.2 mL) was added to dissolve the polymer portion of the microcapsules. Then, 0.8 mL of distilled water was added to allow solubilization of the BSA-FITC. The resulting mixture was sonicated for 90 min at 25 °C and centrifuged at 10,000 rpm for 5 min. The amount of BSA-FITC was analyzed using fluorescence spectroscopy (F-4500, Hitachi, Tokyo, Japan). The measurement conditions were: excitation wavelength 490 nm with bandwidth 2.5 nm; emission wavelength 525 nm with bandwidth 2.5 nm; and response time 2 s. The encapsulation efficiency (E) was defined as follows:

$$E = [(\text{amount of encapsulated BSA-FITC})/(\text{total amount of feed BSA-FITC})] \times 100$$

2.5. Conformational stability of BSA-FITC

The BSA-FITC solution (pH 7.4, PBS) as mentioned in Section 2.4 was collected. As a control, original BSA-FITC solution was prepared. The conformational characteristics of BSA-FITC were measured on a Jasco-720 CD spectrophotometer (Tokyo, Japan).

2.6. BSA-FITC release in vivo

Eight Sprague–Dawley (SD) rats (320–350 g, 8 weeks) were used in the *in vivo* release tests. The rats were housed in sterilized cages with sterile food and water and filtered air, and were handled in a laminar flow hood following aseptic techniques. All animals were treated in accordance with the Catholic University of Korea Council on Animal Care Guidelines. Three formulation types containing 0.5, 1.15 and 2.91 mg/mL of BSA-FITC were used in the *in vivo* release experiments. The F-6 microcapsules (Table 1) had BSA-FITC of 49.3% in BSA-FITC-loaded microcapsules. Just before administration, the 1 mL solution of BSA-FITC-loaded microcapsules (1, 2.33 and 5.91 mg) was prepared with a 20% (w/v) solution of 5% D-mannitol, 2% carboxymethylcellulose and 0.1% Tween 80 as an injection vehicle. One milliliter only, with a pre-determined amount for the BSA-FITC-loaded microcapsule or BSA-FITC solution, was injected

using a 26-gauge needle into the subcutaneous dorsum of rats that had been anesthetized with ethyl ether. For the *in vivo* detection of BSA-FITC, an aliquot of blood was drawn from the tail vein of each rat at specified blood collection times. A 0.3-mL aliquot of blood from the catheterized tail vein was collected in an Eppendorf tube and mixed with 0.2 mL of a 1:499 mixture of heparin and saline, followed by gentle shaking. To obtain plasma, the blood solution was centrifuged at 10,000 rpm for 5 min at room temperature. To the plasma obtained in this way, DW (100 μL), 66 mM EDTA (300 μL), and 50 mM Hepes (pH 7.4) (400 μL) were added. Plasma samples were stored frozen at −20 °C until assayed by fluorescence spectroscopy (F-4500, Hitachi, Tokyo, Japan). To analyze the state of the probe and to examine the reliability of the method, we recorded spectra of BSA-FITC standard solutions of known concentrations of BSA-FITC in blood. The amount of cumulatively released BSA-FITC was calculated by comparison with the standard calibration curves prepared with known concentrations of BSA-FITC. For each group of three rats treated with a particular formulation of BSA-FITC-loaded microcapsules, the release experiment was separately performed on each rat and the results were averaged. The area under the plasma BSA-FITC concentration vs. time curve was calculated as AUC. The relative bioavailability was calculated by comparing AUC of the BSA-FITC-loaded microcapsules to that of BSA-FITC solution only. For detection of the remaining BSA-FITC at 14 and 28 days, each microcapsule was individually removed from the sacrificed rats. It was dissolved in methylene chloride (2 mL) and then water (5 mL). The amount of remaining BSA-FITC was calculated by comparison with the standard calibration curves prepared with known concentrations of BSA-FITC.

2.7. *Image measurement of* in vivo *microcapsules*

An Olympus IX81 microscope (Olympus, Japan) for fluorescence imaging, a Nikon Eclipse 80i (Nikon, Japan) for optical imaging and an S-2250N scanning electron microscope (SEM; Hitachi, Japan) was used to examine the morphology of the *in vivo* microcapsules removed from the rats. For SEM measurement, the microcapsules removed from the rats were immediately mounted on a metal stub pre-cooled in liquid nitrogen. After mounting of the microcapsules, the metal stub was quickly immersed in a liquid nitrogen bath to minimize alteration of the microcapsules. Then, the stub was freeze-dried at −75 °C using a freeze dryer. Once completely dry, the microcapsules on the metal stub were observed by optical microscopy. The sample on the metal stub was then coated with a thin layer of platinum using a plasma-sputtering apparatus (Emitech, K575, Japan) under an argon atmosphere.

2.8. *Histological analysis*

At 1, 2, 3 and 4 weeks after transplantation, the rats were sacrificed and the microcapsules were dissected individually and removed from the subcutaneous dorsum. The microcapsules were prepared for immunohistochemical analysis. The microcapsules were left in place, and the tissues were immediately fixed with 10% formalin and embedded in paraffin wax. Each embedded specimen was then sectioned (4 μm) along the longitudinal axis of the implant and the sections were stained with 6-diamino-2-phenylindoadihydrochloride (DAPI, Sigma, USA), ED1 (mouse Anti rat-CD68, Serotec, UK), CD4 (mouse anti-rat CD4; chemicon, EU) and hematoxylin and eosin (H&E). The staining procedures for DAPI and ED1 were as follows. The slides were washed with PBS-T (0.05% Tween 20 in PBS). The slides were blocked with buffer of 5% BSA (bovine serum albumin, Roche, Germany) and 5% HS (horse serum, Gibco™, Invitrogen) in PBS for 1 h at 37 °C. Sections were incubated with mouse anti rat-CD68 overnight at 4 °C. After washing with PBS-T, the slides were incubated with the secondary antibody (rat anti-mouse Alexa Fluor®594, Invitrogen) for 3 h at room temperature in the dark condition. After washing with PBS-T, the slides were counter stained with DAPI and then mounted with fluorescent mounting solution (DAKO, Denmark). Immunofluorescence images were visualized under an Olympus IX81 microscope equipped with Meta Image Series.

2.9. *Data analysis*

The areas under individual plasma BSA-FITC concentration–time curves for a released time period (AUC_{0-t}) were calculated. Bioavailabilities were determined by dividing the mean AUC value for each BSA-FITC-loaded microcapsule administration by the mean AUC value for direct BSA-FITC solution only administration into subcutaneous dorsum of rats. Statistical analysis of bioavailabilities was performed using Student's *t*-test. ED 1 and CD4 assays were carried out in independent experiments with $n = 16$ for each data point, with data given as the mean and standard deviation (SD). The results were analyzed with one-way ANOVA, using the Prism 3.00 software package (GraphPad Software Inc., San Diego, CA, USA).

3. Results

3.1. *Preparation of microcapsules*

In this work, we used an ultrasonic atomizer to produce BSA-FITC-loaded microcapsules. A poly(D,L-lactic-co-glycolic acid) (PLGA) solution in ethyl acetate and an aqueous solution containing BSA-FITC were mixed in an ultrasonic atomizer, after which the two solutions were fed separately. When two solutions are mixed in the mixing chamber of the nozzle, a water/oil (w/o) emulsion is formed. The time required for the emulsion to pass through the

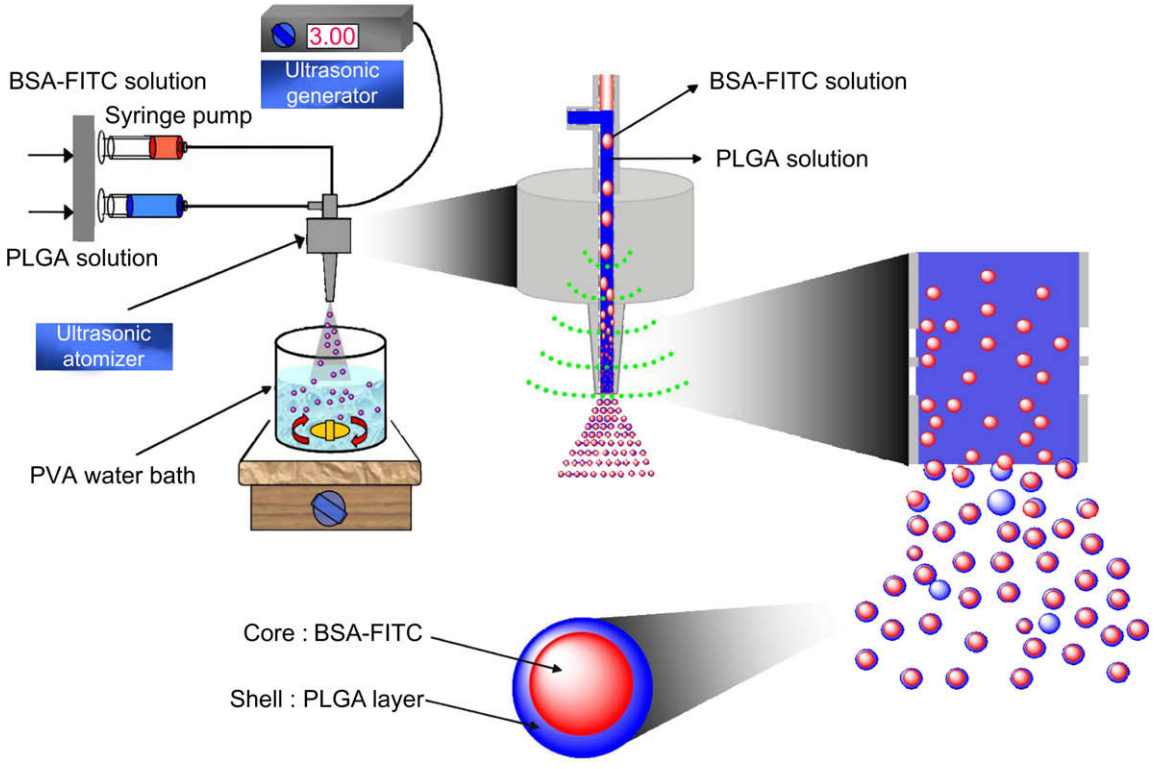

Fig. 1. Schematic depiction of the mono-axial nozzle ultrasonic atomizer microencapsulation method.

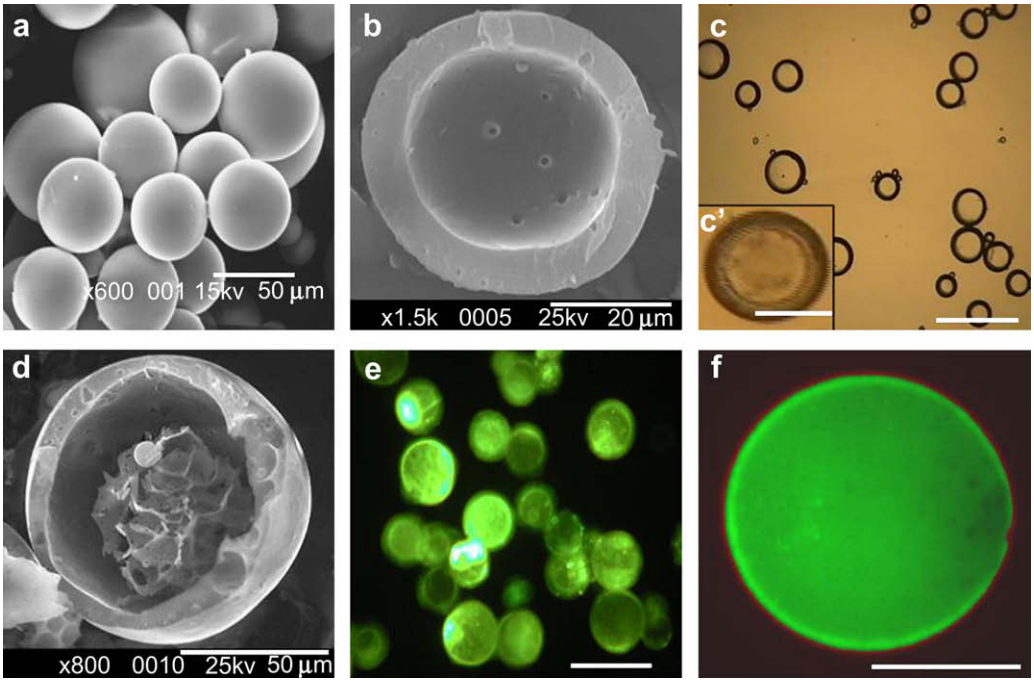

Fig. 2. SEM pictures of freeze-dried microcapsules (a) and a cross-sectioned microcapsule (b). Light microscopy image of microcapsules (c); enlarged image (c′). SEM image of a cross-sectioned BSA-FITC-loaded microcapsule (d). Fluorescence image of BSA-FITC-loaded microcapsules (e). A confocal fluorescence microscopic image of BSA-FITC-loaded microcapsule with Nile Red PLGA (f). Scale bars represent 50 μm (a, d, c′), 20 μm (b, f) and 100 μm (c, e).

mixing part of the nozzle is approximately 5 s. The atomization process results in the formation of emulsion microdroplets inside the nozzle. These aqueous microdroplets become smaller as they are sprayed through the nozzle tip. BSA-FITC-loaded microcapsules surrounded by the PLGA solution were obtained by spraying microdroplets over a water bath containing polyvinyl alcohol (PVA) (Fig. 1).

BSA-FITC encapsulation efficiency and the particle size of BSA-FITC-loaded microcapsules can be related to the flow rate of each solution, the PLGA and PVA concentrations, and sonication power (Table 1). Depending on the conditions, we obtained a BSA-FITC encapsulation efficiency of 20–74% and a particle size of 10–630 μm. From the various outcomes, we sought a manufacturing condition that provided acceptable yields, while minimizing loss of BSA-FITC and PLGA, and optimizing particle size (~50 μm) and encapsulation efficiency (>60%). The F-6 microcapsules (Table 1), which had an encapsulation efficiency of 63% and a uniform particle size of 48 μm (±8 μm), were selected for subsequent *in vivo* release experiments using subcutaneous injection into rats.

3.2. Characterization of microcapsules

Fig. 2 shows images of microcapsules without and with BSA-FITC observed by scanning electron microscopy (SEM), optical microscopy and confocal fluorescence microscopy (CFM). SEM analysis of microcapsules demonstrated that they were spherical with a smooth surface (Fig. 2a). The image of a freeze-dried, fractured microcapsule without BSA-FITC clearly shows the inner empty core surrounded by the PLGA shell (Fig. 2b). The polymer layer covering the aqueous core was also clearly evident in an optical microscopic image of the microcapsules (Fig. 2c, 2c′). A SEM image of a fractured BSA-FITC-loaded microcapsule clearly reveals the BSA-FITC core inside the PLGA shell (Fig. 2d). The CFM image was obtained from a microcapsule formed after adding fluorescent probes to BSA-FITC in aqueous solution and Nile Red mixed with PLGA in ethyl acetate. The BSA-FITC core appears green, while the PLGA shell is red.

3.3. Conformational stability of BSA-FITC

To assess the structural integrity of encapsulated BSA-FITC, we applied circular dichroism (CD) spectroscopy, which had been widely applied to examining the conformation and self-association of BSA-FITC (Fig. 3). We found that the CD spectra of encapsulated BSA-FITC were virtually indistinguishable from that of a native BSA-FITC solution, indicating that the structure of BSA-FITC encapsulated in microcapsules is preserved intact.

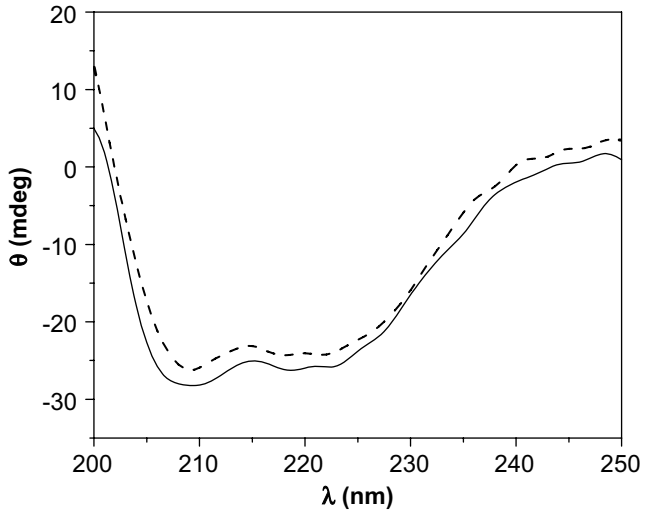

Fig. 3. Far-UV CD spectra of native BSA-FITC (solid line) and encapsulated BSA-FITC (dashed line).

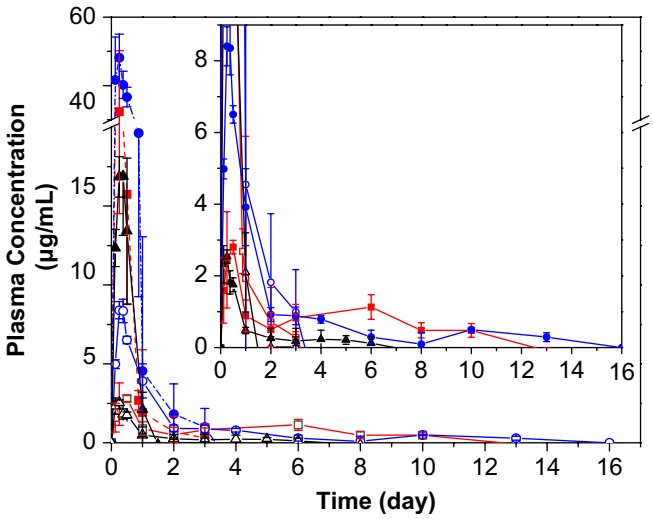

Fig. 4. Time course of BSA-FITC concentration in plasma over 20 days after injection of BSA-TIFC-loaded microcapsules (0.5 mg/mL (–▲–), 1.15 mg/mL (–■–) or 2.91 mg/mL (–●–) and BSA-FITC solution only (0.5 mg/mL (–△–), 1.15 mg/mL (–□–) or 2.91 mg/mL BSA-FITC (–○–).

3.4. *BSA-FITC release* in vivo

To determine *in vivo* BSA-FITC release, BSA-FITC-only solution and BSA-FITC-loaded microcapsules were prepared using different concentrations of BSA-FITC (0.5, 1.15 and 2.91 mg/mL). BSA-FITC release from BSA-FITC-loaded microcapsules *in vivo* was monitored over time by measuring plasma BSA-FITC concentrations in rats using fluorescence spectroscopy (Fig. 4). We detected plasma BSA-FITC for up to 3 days in rats injected with the BSA-FITC-only solution. Plasma BSA-FITC concentrations in these rats reached a maximum after 6 h and then rapidly declined, approaching zero after 2 days. Plasma BSA-FITC concentration in rats injected with BSA-FITC-loaded microcapsules also reached a maximum within 6 h but exhibited a sustained-release profile, producing detectable levels of BSA-FITC in plasma for up to 2 weeks. A larger dose of BSA-FITC produced a larger, more sustained release.

To investigate the reason for the loss of detectable BSA-FITC beyond 2 weeks, we examined BSA-FITC-loaded microcapsules in tissue excised from a rat after 1, 2, 3 and 4 weeks using optical and fluorescence microscopy (Fig. 5). In optical images, spherical microcapsules in the subcutaneous dorsum appeared orange in color owing to the BSA-FITC content of the microcapsules. In both optical and fluorescence images, the orange coloration and fluorescence intensity decreased with implantation time. The steady decrease in fluorescence intensity was attributed to the sustained release of BSA-FITC from the microcapsules. These results indicate that at approximately 2 weeks, the concentration of BSA-FITC in plasma fell to below the limit of detection by fluorescence spectroscopy. The BSA-FITC contents remaining inside the microcapsules after 14 days were 50–60%. After 28 days, the remaining BSA inside the microcapsules decreased to below 30–45%.

AUC_{0-t} values (calculated by measuring the area under the plasma BSA-FITC curves (AUC) from t_0 to time t using the trapezoidal rule) and absolute bioavailability of BSA-FITC were determined from the plasma concentration profiles (Table 2). For BSA-FITC-loaded microcapsules with 0.5, 1.15 and 2.91 mg/mL of BSA-FITC, the AUC_{0-t} was 2.7 ± 0.9, 7.4 ± 4.6 and 13.6 ± 0.6 μg/mL, respectively. The absolute bioavailability of BSA-FITC from BSA-FITC-loaded microcapsules was approximately 22, 38 and 31% from the AUC_{0-t} of the BSA-FITC-only solution at these same BSA-FITC concentrations.

3.5. *Host tissue response*

To assess the biocompatibility of the BSA-FITC-loaded microcapsules, we examined the tissues within and near the transplanted microcapsules. Tissue was stained with DAPI to stain nuclei, and with the macrophage marker ED1 and CD4 to characterize the extent of host cell and inflammatory cell accumulation (Fig. 6). DAPI staining (blue) showed many host cells surrounding the BSA-FITC-loaded microcapsules, ED1 and CD4 staining (red) showed macrophage accumulation at the surfaces of the BSA-FITC-loaded microcapsules and in surrounding tissues. The number of ED1- and CD4-positive cells in tissue adjacent to the microcapsules was greatest at 1 week and then decreased, indicating a marked decline in macrophages over time (Fig. 7). The decline trend of the ED1- and CD4-positive cells matched

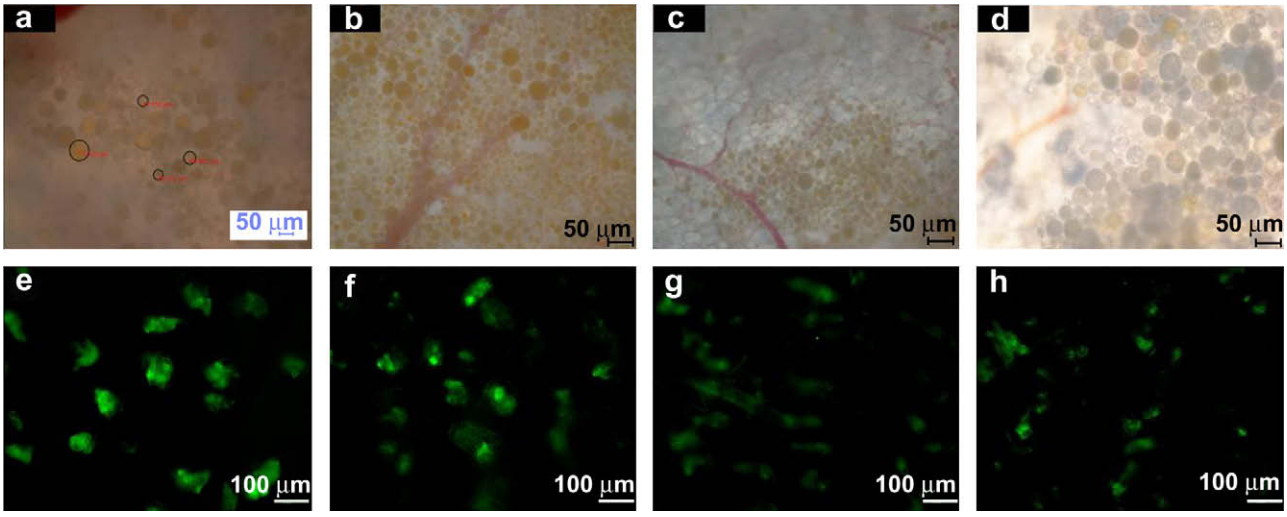

Fig. 5. Optical (upper) and fluorescence (bottom) images of BSA-FITC-loaded microcapsules in tissue excised from a rat after 1 week (a, e), 2 weeks (b, f), 3 weeks (c, g) and 4 weeks (d, h). Scale bars represent 50 μm (a–d) and 100 μm (e–h).

Table 2
Bioavailability of BSA-FITC after subcutaneous inject of BSA-FITC solution only and BSA-FITC loaded microcapsules.

Administration formulation	BSA-FITC concentration (mg)	AUC_{0-t} (μg/mL)	Bioavailability[a] (%)
BSA-FITC loaded microcapsules	0.5	2.7 ± 0.9	21.6 ± 7.5[b]
	1.15	7.4 ± 4.6	37.9 ± 13.7[b]
	2.91	13.6 ± 0.6	30.9 ± 1.4[b]
Administration of BSA-FITC solution only	0.5	12.3 ± 2.9	
	1.15	19.5 ± 3.5	
	2.91	43.9 ± 2.9	

Average represents the mean SD ($n = 3$).
[a] Bioavailability = (mean AUC value for each BSA-FITC loaded microcapsules administration)/(mean AUC value for direct BSA-FITC administration).
[b] $P < 0.01$ versus BSA-FITC solution only.

closely in the surrounding BSA-FITC-loaded microcapsules. In addition, green fluorescence images showed BSA-FITC remaining inside the BSA-FITC-loaded microcapsules. The intensity and area of fluorescence decreased with implantation time. The decreasing intensity of fluorescence in these experiments provides further evidence for the sustained release of BSA-FITC from BSA-FITC-loaded microcapsules.

Hematoxylin and eosin (H&E)-stained histological sections of harvested microcapsules showed that after 1 week the numbers of macrophages and neutrophils had increased in the border zone and near the microcapsules, as well as inside the tissue layer (Fig. 8). Host cells had invaded the microcapsules, and there was a dense accumulation of inflammatory cells around each microcapsule. In agreement with the ED1 and CD4 assay results, the number of inflammatory cells peaked at 1 week and then decreased over time, indicating that the implantation of foreign microcapsules resulted in an acute short-term inflammatory response.

4. Discussion

Microcapsules offer a number of advantages for *in vivo* applications. However, before this technology can achieve widespread use in practical biomedical applications, it is necessary to further simplify the process of manufacturing microcapsules while maintaining their advantages. A number of microencapsulation preparation processes have been described, including solvent extraction/evaporation, phase separation and spray drying [12–15].

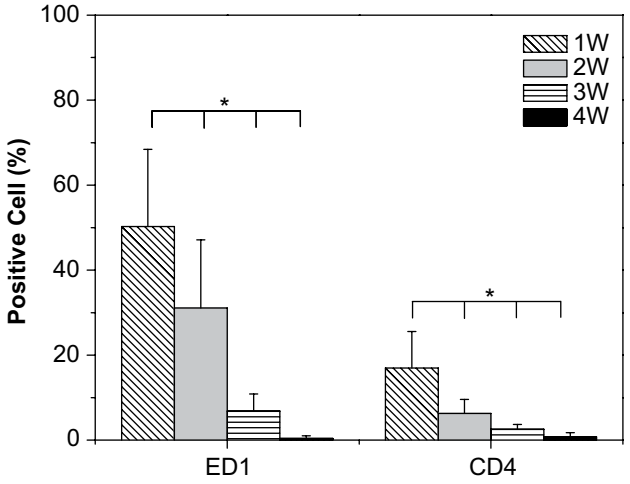

Fig. 7. The number of ED1- and CD4-positive cells on BSA-FITC-loaded microcapsules as a function of time after injection. Statistical analysis was performed using a one way-ANOVA with Bonferroni's multiple comparisons (*$P < 0.01$).

Microcapsules that exhibit a core-shell structure may offer several additional advantages in drug delivery [21,22]. Previous work has reported the production of core-shell microcapsules using a modified co-axial nozzle apparatus that allowed the formation of a dual solution responsible for generating the microcapsules [19,20,23,24]. Although the production of microcapsules using this apparatus is simple and highly efficient [19,20], a newly designed mono-axial nozzle ultrasonic atomizer offers an improved and simplified approach to manufacturing microcapsules. The use of a mono-axial nozzle ultrasonic atomizer to form core-shell microcapsules, described here, has not been previously reported. With this mono-axial nozzle ultrasonic atomizer and a mixture of PLGA and BSA-FITC solutions, BSA-FITC could be microencapsulated through formation of BSA-FITC and PLGA microdroplets within a few seconds. By varying fabrication parameters, such as polymer and protein solution flow rates, PLGA and PVA concentrations, and sonication power, particles with optimal properties can be simply produced. In this work, we have demonstrated that BSA-FITC-loaded microcapsules with a desired particle size can be prepared with relatively high encapsulation efficiency. Unlike conventional microspheres, in which the loaded BSA-FITC is dispersed

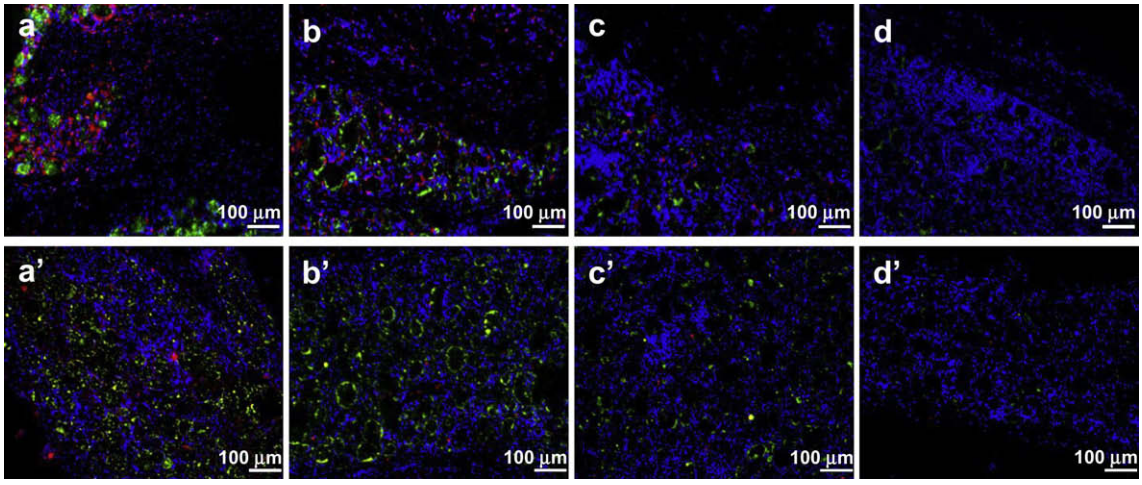

Fig. 6. ED1 and CD4 immunofluorescence staining of BSA-FITC-loaded microcapsules 1 week (a), 2 weeks (b), 3 weeks (c) and 4 weeks (d) after injection. Blue and red correspond to DAPI and, ED1 and CD4 immunohistochemical staining, respectively; green represents FITC from BSA-FITC-loaded microcapsules. Scale bar represents 100 μm.

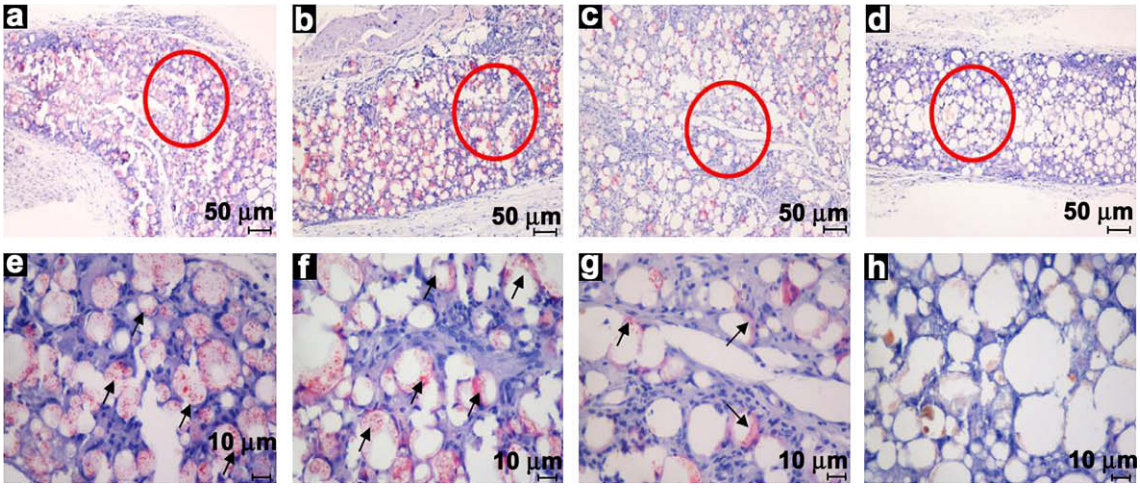

Fig. 8. H&E staining of BSA-FITC-loaded microcapsules 1 week (a, e), 2 weeks (b, f), 3 weeks (c, g), and 4 weeks (d, h) after injection. Bottom images are magnifications of circled areas. The arrows represent inflammatory cells. Magnification is ×100 (top) and ×400 (bottom).

throughout the spherical PLGA sphere, a microcapsule clearly forms an inner BSA-FITC core surrounded by a PLGA shell. It is important to note that the diameters of these microcapsules are less than 100 μm, and thus can be readily injected into the body with comparably less pain [10,11]. The diameters of the microcapsules could be varied over a fairly broad range (10–630 μm) by varying fabrication parameters.

The stability of encapsulated proteins is a particularly important consideration for protein encapsulation processes [25–28]. Currently, physical stability of BSA-FITC during drug loading was evaluated in terms of its conformational change using CD spectroscopy. Such spectral features indicated that the overall conformation of BSA-FITC was not altered after drug loading. Unlike conventional approaches to encapsulating proteins, which typically require vigorous stirring that tends to destroy protein activity, BSA-FITC encapsulated by this method remains stable owing to its limited exposure to a water–organic solvent interface and the mild production conditions used.

For practical *in vivo* application of microcapsules, the desired sustained release from protein-loaded microcapsules must be demonstrated. In contrast to direct injection of a BSA-FITC-only solution, which resulted in a rapid increase in plasma BSA-FITC concentration and complete disappearance within 3 days, BSA-FITC-loaded microcapsules exhibited a fast initial burst on the first day and followed by a sustained release profile. The initial burst release is likely that the BSA-FITC in the PLGA shell layer molecularly dispersed throughout the microcapsules and/or the BSA-FITC from the cracked microcapsules is rapidly perfused by the releasing buffer under biological conditions. Most of the BSA-FITC, however, is present inside the microcapsules and/or the non-cracked microcapsules and is therefore not easily available to the biological media. Thus, BSA-FITC inside the microcapsules is released at a very slow rate for up to 6–14 days.

The concentration and sustainability of BSA-FITC in plasma were dependent on the initial dose of BSA-FITC. BSA-FITC release seemed to cease after approximately 14 days, at which point the measurement of additional BSA-FITC release was hindered by the detection limits of fluorescence spectroscopy. This interpretation is supported by the gradual decrease in intensity of BSA-FITC that remained inside microcapsules.

Our observations thus demonstrate that BSA-FITC-loaded microcapsules may be a promising system for delivering drugs while maintaining drug potency. One crucial prerequisite for the practical *in vivo* application of a microcapsule drug delivery system is an understanding of the potential for a host tissue response after implantation [29–31]. BSA-FITC-loaded microcapsules can induce an inflammatory response, stimulating increased cellular activity and delaying engraftment between host tissue and PLGA microcapsules. Although PLGA is a FDA-approved material that has been widely used in clinical medicine, it eventually degrades directly to acid, leading to undesirable inflammatory responses [32,33] and increasing the susceptibility of PLGA microcapsules to inflammatory damage. One study has suggested that macrophages act primarily at the interface between tissue and foreign materials and have a role in material resorption, although the underlying inflammatory mechanism is still poorly understood [34,35]. We thus evaluated host tissue responses, examining tissue sections from rats injected with BSA-FITC-loaded microcapsules and quantifying the numbers of cells, macrophages, and T cells using DAPI staining, the macrophage marker ED1, and T lymphocyte marker CD4, respectively. ED1, CD4 and H&E staining revealed that the tissues surrounding the PLGA microcapsules contained macrophages and neutrophils. Over time, however, there was a marked decrease in macrophages and neutrophils. Although the inflammation observed surrounding the injected BSA-FITC-loaded microcapsules in rats was most likely caused by specific graft rejection of the PLGA, our findings suggest that these microcapsules may be safe and biocompatible *in vivo*, and thus represent potential candidates for clinical development.

5. Conclusions

Using a mono-axial nozzle ultrasonic atomizer, we prepared BSA-FITC-loaded microcapsules consisting of a BSA-FITC core and a PLGA shell. The advantages of this mono-axial nozzle ultrasonic approach can be summarized as a simple preparation process and less stress on encapsulated proteins. The BSA-FITC-loaded microcapsules were characterized in terms of morphology, particle diameter, and BSA-FITC encapsulation efficiency. A solution containing these microcapsules could be easily injected into rats using a microsurgical needle. Importantly, we observed a sustained release of BSA-FITC from BSA-FITC-loaded microcapsules. Moreover, the initial inflammatory response declined over time. Although the initial burst of BSA-FITC may pose a challenge, we believe the results of the present study provide new options for sustained *in vivo* release of highly potent therapeutics, and represent a useful experimental platform for future protein delivery research.

Acknowledgments

This work was supported by the Korea Science and Engineering Foundation (KOSEF) pioneer grant (M10711060001-08M1106-00110).

Appendix

Figures with essential colour discrimination. Certain figures in this article, in particular Figures 1, 2, 5, 6 and 8, are difficult to interpret in black and white. The full colour images can be found in the on-line version at doi: 10.1016/j.biomaterials.2008.10.030.

References

[1] Hussain A, Arnold JJ, Khan MA, Ahsan F. Absorption enhancers in pulmonary protein delivery. J Control Release 2004;94(1):15–24.
[2] Hamman JH, Enslin GM, Kotzé AF. Oral delivery of peptide drugs: barriers and developments. Biodrugs 2005;19(3):165–77.
[3] Kang J, Schwendeman SP. Pore closing and opening in biodegradable polymers and their effect on the controlled release of proteins. Mol Pharm 2007;4(1):104–18.
[4] Lai M-K, Chang C-Y, Lien Y-W, Tsiang RC-C. Application of gold nanoparticles to microencapsulation of thioridazine. J Control Release 2006;111(3):352–61.
[5] Hoffman AS, Stayton PS. Conjugates of stimuli-responsive polymers and proteins. Prog Polym Sci 2007;32(8–9):922–32.
[6] Emma L-V, Lisbeth G, Victor N, Simon C. In vitro biocompatibility and bioactivity of microencapsulated heparan sulfate. Biomaterials 2007;28(12):2127–36.
[7] Orive G, Tam SK, Pedraz JL, Hallé J-P. Biocompatibility of alginate-poly-L-lysine microcapsules for cell therapy. Biomaterials 2006;27(20):3691–700.
[8] Li F, Xian RQ, Xing JZ, Yoshie M, Shi CW, Yang J, et al. Pharmaceutical and immunological evaluation of a single-dose hepatitis B vaccine using PLGA microspheres. J Control Release 2006;112(1):35–42.
[9] Moioli EK, Hong L, Guardado J, Clark PA, Mao JJ. Sustained release of TGFβ3 from PLGA microspheres and its effect on early osteogenic differentiation of human mesenchymal stem cells. Tissue Eng 2006;12(3):537–46.
[10] Mathew ST, Devi SG, Sandhya KV. Formulation and evaluation of ketorolac tromethamine-loaded albumin microspheres for potential intramuscular administration. AAPS PharmSciTech 2007;8(1):14–22.
[11] Wang X, Wenk E, Hu X, Castro RG, Meinel L, Wang X, et al. Silk coatings on PLGA and alginate microspheres for protein delivery. Biomaterials 2007;28(28):4161–9.
[12] Freitas S, Merkle HP, Gander B. Ultrasonic atomisation into reduced pressure atmosphere – envisaging aseptic spray-drying for microencapsulation. J Control Release 2004;95(2):185–95.
[13] Taluja A, Bae YH. Role of a novel excipient poly(ethylene glycol)-*b*-poly(L-histidine) in retention of physical stability of insulin at aqueous/organic interface. Mol Pharm 2007;4(4):561–70.
[14] Jain RA. The manufacturing techniques of various drug loaded biodegradable poly(lactide-co-glycolide) (PLGA) devices. Biomaterials 2000;21(23):2475–90.
[15] Watts PJ, Davies MC, Melia CD. Microencapsulation using emulsification/solvent evaporation: an overview of techniques and applications. Crit Rev Ther Drug Carrier Syst 1990;7(3):235–59.
[16] Yeo Y, Park K. Control of encapsulation efficiency and initial burst in polymeric microparticle systems. Arch Pharm Res 2004;27(1):1–12.
[17] Degim IT, Celebi N. Controlled delivery of peptides and proteins. Curr Pharm Des 2007;13(1):99–117.
[18] Yeo Y, Basaran OA, Park K. A new process for making reservoir-type microcapsules using ink-jet technology and interfacial phase separation. J Control Release 2003;93(2):161–73.
[19] Yeo Y, Park K. A new microencapsulation method using an ultrasonic atomizer based on interfacial solvent exchange. J Control Release 2004;100(3):379–88.
[20] Yeo Y, Park K. Characterization of reservoir-type microcapsules made by the solvent exchange method. AAPS PharmSciTech 2004;5(4):e52.
[21] Darrabie MD, Kendall Jr WF, Opara EC. Characteristics of poly-L-ornithine-coated alginate microcapsules. Biomaterials 2005;26(34):6846–52.
[22] Jovanovic AV, Flint JA, Varshney M, Morey TE, Dennis DM, Duran RS. Surface modification of silica core-shell nanocapsules: biomedical implications. Biomacromolecules 2006;7(3):945–9.
[23] Hwang YK, Jeong U, Cho EC. Production of uniform-sized polymer core-shell microcapsules by coaxial electrospraying. Langmuir 2008;24(6):2446–51.
[24] Pollauf EJ, Pack DW. Use of thermodynamic parameters for design of double-walled microsphere fabrication methods. Biomaterials 2006;27(14):2898–906.
[25] Pérez C, Castellanos IJ, Costantino HR, Al-Azzam W, Griebenow K. Recent trends in stabilizing protein structure upon encapsulation and release from bioerodible polymers. J Pharm Pharmacol 2002;54(3):301–13.
[26] Lee KY, Yuk SH. Polymeric protein delivery systems. Prog Polym Sci 2007;32(7):669–97.
[27] Jin T, Zhu J, Wu F, Yuan W, Geng LL, Zhu H. Preparing polymer-based sustained-release systems without exposing proteins to water–oil or water–air interfaces and cross-linking reagents. J Control Release 2008;128(1):50–9.
[28] Weiner AA, Bock EA, Gipson ME, Shastri VP. Photocrosslinked anhydride systems for long-term protein release. Biomaterials 2008;29(15):2400–7.
[29] Ho T-Y, Chen Y-S, Hsiang C-Y. Noninvasive nuclear factor-κB bioluminescence imaging for the assessment of host–biomaterial interaction in transgenic mice. Biomaterials 2007;28(30):4370–7.
[30] Burugapalli K, Pandit A. Characterization of tissue response and in vivo degradation of cholecyst-derived extracellular matrix. Biomacromolecules 2007;8(11):3439–51.
[31] Kim MS, Ahn HH, Shin YN, Cho MH, Khang G, Lee HB. An in vivo study of the host tissue response to subcutaneous implantation of PLGA- and/or porcine small intestinal submucosa-based scaffolds. Biomaterials 2007;28(34):5137–43.
[32] Hickey T, Kreutzer D, Burgess DJ, Moussy F. Dexamethasone/PLGA microspheres for continuous delivery of an anti-inflammatory drug for implantable medical devices. Biomaterials 2002;23(7):1649–56.
[33] Jilek S, Walter E, Merkle HP, Corthesy B. Modulation of allergic responses in mice by using biodegradable poly(lactide-co-glycolide) microspheres. J Allergy Clin Immunol 2004;114(4):943–50.
[34] Esposito M, Kennergren C, Holmström N, Nilsson S, Eckerdal J, Thomsen P. Morphologic and immunohistochemical observations of tissues surrounding retrieved transvenous pacemaker leads. J Biomed Mater Res 2002;63(5):548–58.
[35] Benghuzzi H. Cytological evaluation of capsular tissue surrounding TCPL implant in adult rats. Biomed Sci Instrum 1996;32:81–6.